ISSN 2278-3091
Volume 9, No.4, July – August 2020
International Journal of Advanced Trends in Computer Science and Engineering
Available Online at http://www.warse.org/IJATCSE/static/pdf/file/ijatcse119942020.pdf
https://doi.org/10.30534/ijatcse/2020/119942020

A Systematic Methodology to Modify Color Images for Dichromatic Human Color Vision and its Application in Art Paintings

Anastasios Rigos[1], Stamatis Chatzistamatis[2], George E. Tsekouras[3*]
Department of Cultural Technology and Communication, University of the Aegean, Mytilene, Greece
[1]a.rigos@aegean.gr, [2]stami@aegean.gr [3]gtsek@ct.aegean.gr
[*]corresponding author

ABSTRACT

This paper introduces a systematic methodology to perform image recoloring for color-blind people that suffer from dichromacy, i.e. protanopia, deuteranopia, and tritanopia. The method is applied in digitized art paintings to alleviate accessibility problems related to art content consumption by the color-blind people, which is a very important issue. The methodology involves the RGB, the LMS, and the CIELab color spaces and comprises several steps implemented in sequence. To reduce the computational complexity, the colors of the original image are clustered. Each cluster center is a color. By using a standard technique, the cluster centers are transformed to simulate the effects of protanopia, deuteranopia, and tritanopia. To this end, a specialized objective function is minimized to recolor only the cluster centers that are significantly different from the respective simulated ones, because only these colors are confused by the color-blind. Finally, all colors of the original image belonging to the clusters associated with centers that have been recolored are appropriately recolored, also. The effectiveness of the proposed method is quantified in terms of comparative analysis over several experimental cases.

Key words: Color-blind, dichromacy, image recoloring, objective function, digitized art paintings.

1. INTRODUCTION

The human eye perceives the color using specialized photoreceptor cells, called “cones”, contained in the eye’s retina. There are three types of cones namely, the L-cones, the M-cones, and the S-cones. These cone types are sensitive to different, but overlapping, regions of the visible spectrum [1]. As an approximation of their stimulation, the L-cones correspond to red color, the M-cones to green color, and the S-cones to blue color [2, 3, 4]. Figure 1 depicts the spectral sensitivity distributions for each cone type as reported in [1].

Dysfunction or absence of two or more types of cones results in color vision deficiency (CVD), also known as color blindness (CB) [1, 3, 5]. People suffering from strong CVDs are subjected to various challenges in their everyday life, e.g. road signs and traffic light recognition, object recognition in images, consumption of colored multimedia content, etc. Since the 8% of men and 0.8% of women are color-blind, it is clearly understood that any computational framework that assists the color blindness would be of great importance.

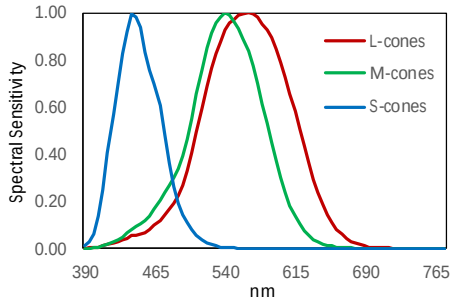

Figure 1: The cones’ spectral sensitivities as functions of the wavelength (in nm) [1].

Depending on the cone types that have been affected, there exist three general classes of CVDs namely, monochromacy (known as achromatopsia), dichromacy, and anomalous trichromacy [1, 3]. Monochromacy (i.e. total color blindness) is the most severe CVD concerning the absence of two or three types of cones, and it is the rarest one. Dichromacy concerns the absence of one type of cones and includes three categories of CVD: (a) the protanopia caused by the absence of the L-cones, (b) the deuteranopia caused by the absence of M-cones, and the tritanopia where the S-cones are missing. Anomalous trichromacy includes three categories namely, protanomaly, deuteranomaly and tritanomaly caused by malfunctioning of the L, M, and S cones, respectively.

Color image analysis has been effectively employed in assisting visually impaired people [6]. In particular, the main strategies to alleviate the CVD effects concern the recoloring of the original image under certain requirements such as image naturalness and color contrast enhancement [3]. Image naturalness focuses on minimizing the perceptual difference between the original and the recolored image. On the other hand, enhancing the color contrast would be very convenient in supporting the object recognition performed by the color blind.

Huang et al [4] used the CIELab color space and developed a rotation mechanism to transform the original color in the recolored one. To accomplish this, they designed an objective function, which quantified the naturalness and the contrast requirements. In this direction, Jeong et al [5] substantially improved the previous recoloring process by performing a translation of the colors not perceived correctly by the color-blind in distinguishable RGB color regions. Hassan and Paramersan [7] used the XYZ color space to carry out image enhancement in three steps namely, normalization, angular color rotation, and color un-normalization. In [8], an optimization algorithm was proposed that was able to preserve the distances between the original colors and the corresponding colors as seen by the color blind. Huang et al [9] performed the color enhancement by extracting key colors and determining an optimal mapping to maintain the contrast between pairs of those colors. Tsekouras et al [10] used evolutionary computation to elaborate on the set of the distinct image colors, which were modified by a daltonization approach to generate the recolored image. In [11], a semantic segmentation procedure was developed to identify semantic image information. Then, the recoloring process was based exclusively on that information. Lin et al [12] obtained the recolored image by developing a robust color separation algorithm to perform eigenvector processing in an opponent color space. Finally, Wong and Bishop [13] proposed an adaptive technique, which was based on non-linear hue remapping able to preserve the image aesthetics.

Although too much effort has been put in developing natural image recoloring [4, 5, 7, 8, 9, 12, 13], there are relatively few methods that concern art images [10, 11]. Due to the complexity of such kind of images, maintaining a color natural appearance of the recolored image is a very challenging problem [11]. However, the accessibility of color-blind people in cultural content, such as art paintings, has been acknowledged as an important demand by worldwide organizations dealing with the CVDs and cultural organizations such as museums [14, 15, 16]. Many color-blind people are at a disadvantage when choosing to study or enjoy art paintings because they can only discern a confusing set of objects and colors.

In this paper we propose a systematic methodology to produce improved recolored images that maintain the naturalness and contrast enhancement requirements for the test case of digitized art paintings. In a nutshell, colors that are not perceived correctly by the color-blind are detected and elaborated. Then, a specialized objective function is minimized to modify the above-mentioned colors so that they can be correctly perceived, and the objects contained in the image can be easily recognized.

The rest of the paper is organized as follows. Section 2 analytically describes the proposed methodology. In Section 3, the simulation experiments are presented and discussed. Finally, the paper concludes in Section 4.

2. THE PROPOSED RECOLORING METHOD

The proposed methodology refers to all cases of dichromacy CVD, i.e. protanopia, deuteranopia, and tritanopia. It involves three color spaces namely, the RGB, the CIELab, and the LMS. In what follows, X_{RGB}, X_{Lab}, and X_{LMS} denote the RGB, the CIELab, and the LMS color spaces. The mapping from X_{RGB} to X_{Lab} is $f: X_{RGB} \to X_{Lab}$, while the mapping from X_{RGB} to X_{LMS} is $g: X_{RGB} \to X_{LMS}$. To carry out the above mappings, the colors are appropriately gamma-corrected, the XYZ color space is used as an intermediate space, and the whole approach is based on the CIE Standard Illuminant D65. More information about the above mappings can be found in [17, 18, 19, 20].

Brettel et al [2] developed an algorithmic framework to simulate the dichromatic human vision. They dealt with all dichromacy cases, i.e. protanopia, deuteranopia, and tritanopia, and showed that a dichromat can see only a subspace of the X_{RGB}. Herein, that subspace is denoted as $X_{RGB,D} \subset X_{RGB}$, where the subscript D indicates the dichromacy and therefore, it interchangeably refers to protanopia, deuteranopia, and tritanopia. To determine $X_{RGB,D}$, they performed specialized transformations that involved the XYZ and LMS color spaces, and came up with a matrix-based mapping denoted as $h: X_{RGB} \to X_{RGB,D}$. Thus, given a color $\boldsymbol{c} \in X_{RGB}$, the dichromat perceives it as $\boldsymbol{c}_D \in X_{RGB,D}$, with $\boldsymbol{c}_D = h(\boldsymbol{c})$. For a detailed description of the above-mentioned color simulation procedure, more information can be found in [2].

The proposed image recoloring methodology consists of several steps applied in sequence. These steps are analytically described in the following paragraphs.

First, we perform cluster analysis on the colors of the original image. Clustering has been effectively used in many applications [21, 22]. Herein, it is used to significantly reduce the color information involved in the computational procedure and ultimately, reduce its complexity. Let us assume that the size of the original image I is $N \times M$. The set of colors of I is denoted as I_{RGB} with $I_{RGB} \subset X_{RGB}$. Since the CIELab color space preserves the Euclidean distances between colors, the set I_{RGB} is mapped in the CIELab space: $I_{Lab} = f(I_{RGB})$, i.e. $I_{Lab} \subset X_{Lab}$. Then, the well-known fuzzy c-means is applied over the set I_{Lab} to partition it into n fuzzy clusters with centers $\boldsymbol{x}_1, \boldsymbol{x}_2, ..., \boldsymbol{x}_n$, where $\forall i: \boldsymbol{x}_i \in X_{Lab}$ (note that in general $\boldsymbol{x}_i \notin I_{Lab}$).

The above-mentioned cluster centers are mapped in the space X_{RGB}: $\forall i \in \{1, 2, ..., n\}: \boldsymbol{y}_i = f^{-1}(\boldsymbol{x}_i)$ with $\boldsymbol{y}_i \in X_{RGB}$ (note that in general $\boldsymbol{y}_i \notin I_{RGB}$). Given $\boldsymbol{y}_i$, its simulation to the color perceived by a protanope, deuteranope or tritanope is denoted as $\boldsymbol{y}_{i,D} = h(\boldsymbol{y}_i)$. By defining a small integer

$\theta << 255$ the next condition is checked: $\forall i \in \{1,2,...,n\} : \left\| \boldsymbol{y}_i - \boldsymbol{y}_{i,D} \right\| \le \theta$.

If the above condition is true, the color $\boldsymbol{y}_i$ is not much different from the $\boldsymbol{y}_{i,D}$, meaning that a dichromat can perceive it correctly and to distinguish it from other colors. Thus, this color remains intact. On the other hand, if the condition is false, the color $\boldsymbol{y}_i$, and all colors in the I_{RGB} that belong to the respective fuzzy cluster, will be recolored. Thus, the set $Y = \{\boldsymbol{y}_1, \boldsymbol{y}_2, ..., \boldsymbol{y}_n\}$ is divided into two subsets, the subset $V = \{\boldsymbol{v}_1, \boldsymbol{v}_2, ..., \boldsymbol{v}_{n_1}\}$, which includes the elements of *Y* that will be recolored, and the subset $U = \{\boldsymbol{u}_1, \boldsymbol{u}_2, ..., \boldsymbol{u}_{n_2}\}$, which includes all the elements of *Y* that will remain intact. Thus, $V \cap U = \varnothing$, $Y = V \oplus U$ and $n_1 + n_2 = n$. The simulated sets *V* and *U* as perceived by the dichromats are $V_D = \{\boldsymbol{v}_{1,D}, \boldsymbol{v}_{2,D}, ..., \boldsymbol{v}_{n_1,D}\}$ and $U_D = \{\boldsymbol{u}_{1,D}, \boldsymbol{u}_{2,D}, ..., \boldsymbol{u}_{n_2,D}\}$ with $V_D \subset X_{RGB,D}$, $U_D \subset X_{RGB,D}$, $\boldsymbol{v}_{i,D} = h(\boldsymbol{v}_i)$, and $\boldsymbol{u}_{j,D} = h(\boldsymbol{u}_j)$.

The objective is to calculate a recoloring set $V_{rec} = \{\boldsymbol{v}_{rec,1}, \boldsymbol{v}_{rec,2} ... \boldsymbol{v}_{rec,n_1}\}$ of the set *V*. Since the X_{LMS} space is directly related to the behavior of the cones, the impact of their absence or dysfunctionality is well quantified in that space. Therefore, the set *V* is mapped in X_{LMS} as: $g(V) = \{g(\boldsymbol{v}_1), g(\boldsymbol{v}_2), ..., g(\boldsymbol{v}_{n_1})\}$ with $g(\boldsymbol{v}_i) \in X_{LMS}$ $\forall i \in \{1,2,...,n_1\}$. The same is done for V_D, which gives the set $g(V_D) = \{g(\boldsymbol{v}_{1,D}), g(\boldsymbol{v}_{2,D}), ..., g(\boldsymbol{v}_{n_1,D})\}$ with $g(\boldsymbol{v}_{i,D}) \in X_{LMS}$ $\forall i \in \{1,2,...,n_1\}$.

In the LMS space, the error between the color $g(\boldsymbol{v}_i)$ and its simulation $g(\boldsymbol{v}_{i,D})$ is: $\boldsymbol{e}_i = g(\boldsymbol{v}_i) - g(\boldsymbol{v}_{i,D})$, and the recoloring of $g(\boldsymbol{v}_i)$ is determined by a procedure similar to the one developed in [10],

$$g(\boldsymbol{v}_{rec,i}) = g(\boldsymbol{v}_i) + \Lambda_{D,i}\, \boldsymbol{e}_i \tag{1}$$

with
$$\Lambda_{D,i} = \begin{bmatrix} 1 & \lambda_{D,i,12} & \lambda_{D,i,13} \\ \lambda_{D,i,21} & 1 & \lambda_{D,i,23} \\ \lambda_{D,i,31} & \lambda_{D,i,32} & 1 \end{bmatrix} \tag{2}$$

where $i = 1,2,...,n_1$. For protanopia, the implementation of (1) along with the respective matrix in (2) leads to a reduction of the L in favor of M and S, obtaining less saturated red/oranges and more saturated greens, increasing the contrast and therefore, decreasing color confusion of a protanope viewer. In the case of deuteranopia, the above process leads to the reduction of green in favor of red and blue colors obtaining similar results. Finally, the above mechanism appears to have a similar effect for the case of tritanopia. In all cases, the color confusion is alleviated.

For protanopia, $\lambda_{D,i,12} = \lambda_{D,i,13} = 0$, while the rest four parameters will be evaluated by the optimization process that follows. For deuteranopia, $\lambda_{D,i,21} = \lambda_{D,i,23} = 0$, while the rest of the parameters will be adjusted by the optimization procedure that follows. Finally, for tritanopia $\lambda_{D,i,31} = \lambda_{D,i,32} = 0$ while the rest of the parameters will be treated similarly as in the previous cases.

To this end, the recolored color in the RGB space is obtained as $\boldsymbol{v}_{rec,i} = g^{-1}(g(\boldsymbol{v}_{rec,i}))$. In addition, its dichromacy simulation is calculated according to the following mapping: $\boldsymbol{v}_{rec,i,D} = h(\boldsymbol{v}_{rec,i})$ $i = 1,2,...,n_1$.

The set that contains the recolored elements of *V* is denoted as $V_{rec} = \{\boldsymbol{v}_{rec,1}, \boldsymbol{v}_{rec,2}, ..., \boldsymbol{v}_{rec,n_1}\}$, while its dichromacy simulation as $V_{rec,D} = \{\boldsymbol{v}_{rec,1,D}, \boldsymbol{v}_{rec,2,D}, ..., \boldsymbol{v}_{rec,n_1,D}\}$.

The elements of the sets $V, V_{rec}, V_{rec,D}, U$, and U_D are mapped into the X_{Lab} space and the following sets are derived:

$$f(V) = \{f(\boldsymbol{v}_1), f(\boldsymbol{v}_2), ..., f(\boldsymbol{v}_{n_1})\} \tag{4}$$
$$f(V_{rec}) = \{f(\boldsymbol{v}_{rec,1}), f(\boldsymbol{v}_{rec,2}), ..., f(\boldsymbol{v}_{rec,n_1})\} \tag{5}$$
$$f(V_{rec,D}) = \{f(\boldsymbol{v}_{rec,1,D}), f(\boldsymbol{v}_{rec,2,D}), ..., f(\boldsymbol{v}_{rec,n_1,D})\} \tag{6}$$
$$f(U) = \{f(\boldsymbol{u}_1), f(\boldsymbol{u}_2), ..., f(\boldsymbol{u}_{n_2})\} \tag{7}$$
$$f(U_D) = \{f(\boldsymbol{u}_{1,D}), f(\boldsymbol{u}_{2,D}), ..., f(\boldsymbol{u}_{n_2,D})\} \tag{8}$$

The main objective of the proposed method is to optimize the parameters of the matrices $\Lambda_{D,i}$ (with $i = 1,2,...,n_1$) so that the recoloring process in eq. (1) will satisfy the requirements of naturalness and contrast enhancement. To accomplish this task, we follow an approach similar to the one developed by Chatzistamatis et al in [10].

Considering the sets $f(V)$ and $f(U)$, the distances between their elements $\left\| f(\boldsymbol{v}_i) - f(\boldsymbol{u}_j) \right\|$ $(1 \le i \le n_1 ; 1 \le j \le n_2)$ concern the color differences as perceived by a normal viewer.

After the recoloring process the respective differences as perceived by a dichromat viewer concern the sets $f(V_{rec,D})$ and $f(U_D)$ where the distances between their elements are $\left\| f\left(\boldsymbol{v}_{rec,i,D}\right) - f\left(\boldsymbol{u}_{j,D}\right) \right\|$. The objective is to keep the above distances as similar as possible, so that the dichromat will be able to perceive the differences between colors in a similar way as the normal color vision viewer. Thus, summing over all pairs,

$$S_1 = \frac{1}{n_1 n_2} \sum_{i=1}^{n_1} \sum_{j=1}^{n_2} \left\| \left\| f(\boldsymbol{v}_i) - f(\boldsymbol{u}_j) \right\| - \left\| f\left(\boldsymbol{v}_{rec,i,D}\right) - f\left(\boldsymbol{u}_{j,D}\right) \right\| \right\| \tag{9}$$

Following the same approach for the sets $f(V)$ and $f(V_{rec,D})$ we arrive at

$$S_2 = \frac{1}{n_1^2}\sum_{i=1}^{n_1}\sum_{j=1}^{n_1}\left\| f(\boldsymbol{v}_i) - f(\boldsymbol{v}_j)\right\| - \left\| f\left(\boldsymbol{v}_{rec,i,D}\right) - f\left(\boldsymbol{v}_{rec,j,D}\right)\right\| \quad (10)$$

It can be easily seen that the minimization of J_1 and J_2 obtains a recoloring image, the dichromatic perception of which retains the contrast of the original one.

To satisfy naturalness, the objective function is

$$S_3 = \frac{1}{n_1}\sum_{i=1}^{n_1}\left\| f(\boldsymbol{v}_i) - f(\boldsymbol{v}_{rec,i})\right\| \quad (11)$$

Eq. (11) can be easily interpreted since we wish the modified colors to be close to the original ones.

To this end, the overall objective function reads as

$$J = S_1 + S_2 + \varphi S_3 \quad (12)$$

where φ is a regularization parameter that takes positive values and is used to obtain a counterbalance between the distinct parts of the objective function.

To summarize, the main objective of the proposed methodology is to minimize the function *J* with respect to the elements of the matrices $\Lambda_{D,i}$ (with $i = 1, 2, ..., n_1$).

Specifically, for the case of protanopia the parameters are $\lambda_{D,i,21}, \lambda_{D,i,23}, \lambda_{D,i,31}, \lambda_{D,i,32}$, for deuteranopia $\lambda_{D,i,12}$, $\lambda_{D,i,13}$, $\lambda_{D,i,31}, \lambda_{D,i,32}$, and for tritanopia $\lambda_{D,i,12}, \lambda_{D,i,13}$, $\lambda_{D,i,21}, \lambda_{D,i,23}$. Thus, for each of the above cases there are n_1 matrices, and for each matrix 4 parameters. Therefore, in all dichromatic cases there exist $4n_1$ parameters to be optimized. To perform the optimization, we use the differential evolution (DE) algorithm [23]. The DE comprises three evolving learning phases: the mutation, crossover and selection. Two parameters must be defined namely, the $F_R \in (0, 1]$ that controls the rate at which the population evolves, and the $C_R \in [0, 1]$ that controls the fraction of the parameter values copied from one generation to the next.

The optimization obtains the parameters of the matrices $\Lambda_{D,i}$ $(i = 1, 2, ..., n_1)$ that minimize the function *J*. Each matrix corresponds to one color of the set *V*.

Recalling that the elements of *V* were recolored, and $\boldsymbol{v}_i \in V$ corresponds to the cluster center $f(\boldsymbol{v}_i)$ in the CIELab space, we must accordingly recolor all colors of the original image that belong to the fuzzy cluster the center of which is the color $f(\boldsymbol{v}_i)$. We denote the subset of colors of I_{RGB} that belong to that cluster as C_i (with $C_i \subset I_{RGB}$). Note that $i = 1, 2, ..., n_1$, and it refers to the color elements of the set *V* because only these colors were recolored by the optimization process. Let assume that $\boldsymbol{c}_\ell \in C_i$ is the color of the pixel $\boldsymbol{p}_{kt}$ $(1 \le k \le N; 1 \le t \le M)$ of the original image *I*. Its simulated vector is $\boldsymbol{c}_{\ell,D} = h(\boldsymbol{c}_\ell)$. Both the above colors are mapped in the X_{LMS} space to get the vectors $g(\boldsymbol{c}_\ell)$ and $g(\boldsymbol{c}_{\ell,D})$. Then, depending on the dichromacy CVD and using the matrix $\Lambda_{D,i}$ that corresponds to $\boldsymbol{v}_i$ (i.e. to C_i), we apply eq. (1) to obtain the recolored color in the LMS space, which is denoted as $g(\boldsymbol{c}_{rec,\ell})$. Thus, the recoloring of $\boldsymbol{c}_\ell$ in the RGB space is obtained as: $\boldsymbol{c}_{rec,\ell} = g^{-1}(g(\boldsymbol{c}_{rec,\ell}))$. Finally, the pixels of the original image that correspond to colors belonging to fuzzy clusters associated with the elements of the set *U* remain intact.

Figure 2: Testing paintings[1]: (a) Painting 1 (by Paul Gauguin), (b) Painting 2 (by Vincent van Gogh), (c) Painting 3 (by Paul Signac), (d) Painting 4 (by Terence Clarke), (e) Painting 5 (by Ljubomir Aleksandrovic), and (f) Painting 6 (by Achilleas Aivazoglou).

Figure 3: Dichromacy simulation paintings using the method of Brettel et al [2]: (a) Tritanopia simulation of Painting 1, (b) Deuteranopia simulation of Painting 2, (c) Tritanopia simulation of Painting 3, (d) Deuteranopia simulation of Painting 4, (e) Protanopia simulation of Painting 5, and (f) Protanopia simulation of Painting 6.

[1] The paintings were taken from the Web Gallery of Art in https://www.wga.hu/ and the Pallet Art in https://paletaart2.wordpress.com/

3. SIMULATION EXPERIMENTS

In this section the proposed algorithm is evaluated for the test cases of six digitized art paintings depicted in Figure 2. The respective simulated paintings using the method of Brettel et al [2] for different dichromacy cases are depicted in Figure 3.

The proposed algorithmic framework is compared to two methods that also deal with protanopia, deuteranopia, and tritanopia. The first method was developed by Huang et al in [9], while the second one was introduced by Wong and Bishop in [13].

To conduct the experiments we set $\theta = 21$, which implies that all colors belonging to a sphere with radius 21 are considered similar to the color located at the center of that sphere. The number of clusters was preselected as n=24 for all the experiments. Regarding eq. (12), we set $\varphi = 0.1$. The domain of values for the optimizing parameters of the matrices in eq. (2) was the interval [0, 1]. The above values were selected by trial-and-error. For the differential evolution: $F_R = 0.8$, $C_R = 0.9$, the population size was equal to 20, and the maximum number of iterations $t_{\max} = 200$.

For the other two methods, the parameter setting was the same as reported in the respective references.

Figures 4-6 illustrate the behavior of the objective function J during the implementation of the differential evolution algorithm for all dichromacy cases and all paintings. Based on these figures, it can be easily concluded that the convergence of the objective function is smooth and fast.

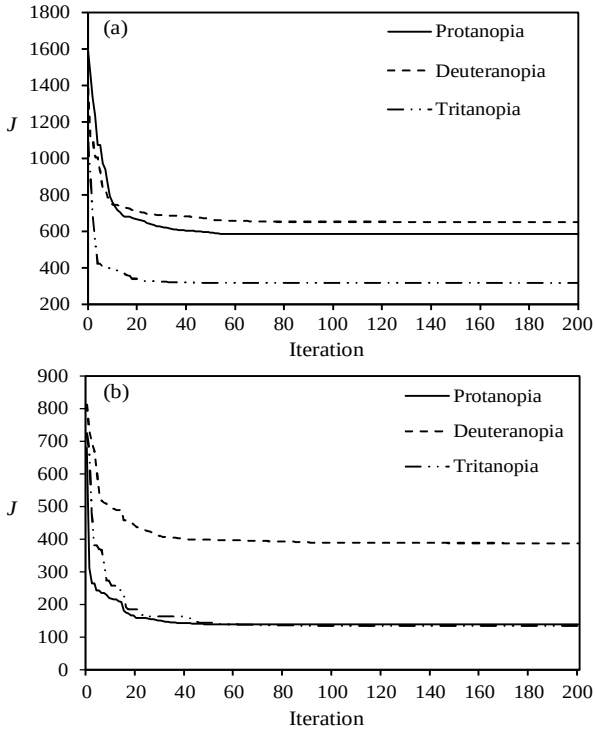

Figure 4: The behavior of J as a function of the iteration number considering the three cases of dichromacy for: (a) Painting 1, and (b) Painting 2.

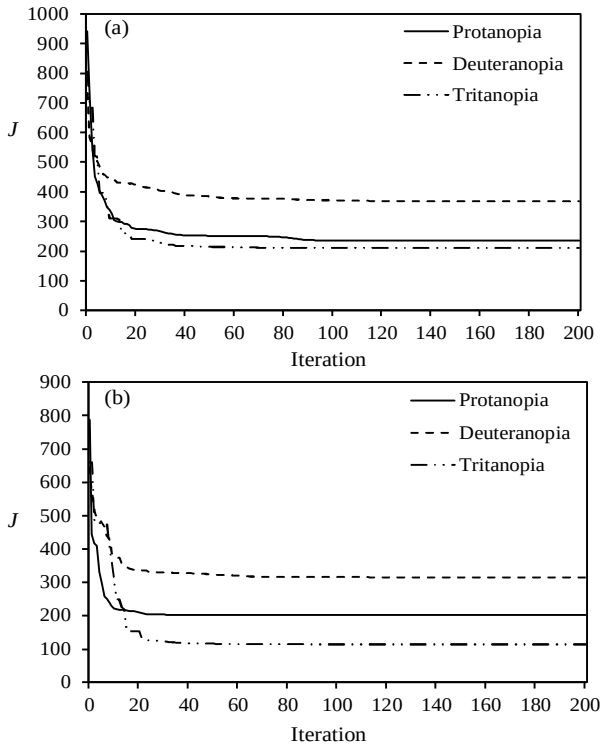

Figure 5: The behavior of J as a function of the iteration number considering the three cases of dichromacy for: (a) Painting 3, and (b) Painting 4.

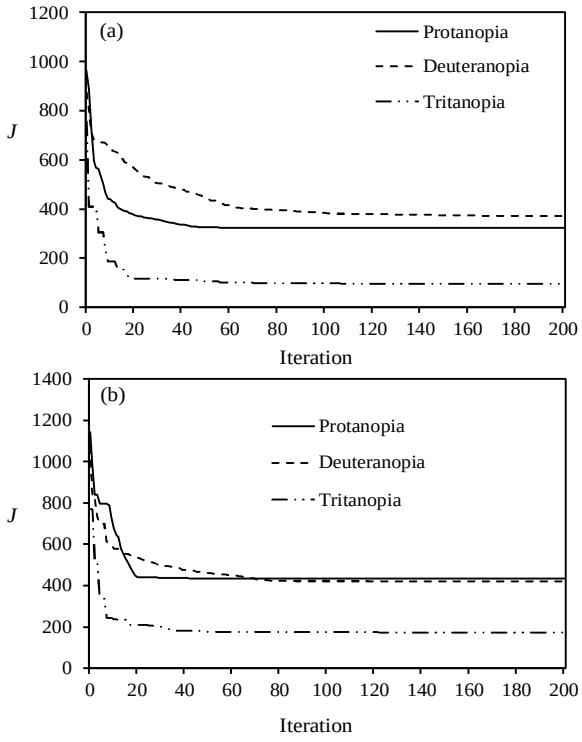

Figure 6: The behavior of J as a function of the iteration number considering the three cases of dichromacy for: (a) Painting 5, and (b) Painting 6.

Note that, in general, the smaller convergent values of J arise in the case of tritanopia, while for protanopia and deuteranopia are, pretty much, of equivalent size. This observation can be justified by the fact that the blue color is

not the dominant color in the paintings of Figure 2. Thus, the cardinality of the set V is small resulting in small values of the individual parts of the function J, as reported in eqs (9)-(11).

The next experiment concerns the naturalness evaluation of the recolored image. For an image of size $N \times M$ the naturalness is quantified by the index studied in [11], which is a modified version of the index developed in [4],

$$E_{nat} = \frac{1}{N\,M} \sum_{k=1}^{N} \sum_{t=1}^{M} \left\| \boldsymbol{p}_{kt} - \boldsymbol{p}_{rec,kt} \right\| \tag{13}$$

where $\boldsymbol{p}_{kt}$ is a pixel of the original image. Smaller values of the above index result in better performance as far as the naturalness of the recolored image is concerned.

Table 1: Naturalness index for the case of protanopia

Painting	Huang et al [9]	Wong and Bishop [13]	Proposed
Painting 1	19.124	22.533	**7.698**
Painting 2	12.439	**9.038**	12.745
Painting 3	29.245	31.691	**24.013**
Painting 4	15.060	24.436	**3.964**
Painting 5	25.488	20.098	**15.585**
Painting 6	35.033	24.833	**8.636**

Table 2: Naturalness index for the case of deuteranopia

Painting	Huang et al [9]	Wong and Bishop [13]	Proposed
Painting 1	9.938	22.533	**6.381**
Painting 2	6.511	9.038	**4.417**
Painting 3	47.346	31.691	**16.337**
Painting 4	11.241	24.436	**3.404**
Painting 5	17.310	20.098	**9.588**
Painting 6	32.455	**22.086**	24.833

Table 3: Naturalness index for the case of tritanopia

Painting	Huang et al [9]	Wong and Bishop [13]	Proposed
Painting 1	78.731	23.811	**18.795**
Painting 2	21.423	11.630	**6.986**
Painting 3	29.874	24.669	**23.545**
Painting 4	30.920	35.964	**6.345**
Painting 5	26.431	34.099	**10.633**
Painting 6	38.195	**7.342**	15.307

Tables 1-3 depict the values of the naturalness index in eq. (13) obtained by the three methods for protanopia, deuteranopia and tritanopia and all paintings. The best values for each simulation are presented in bold fonts.

The results reported in those tables indicate that in most of the experimental simulations, the proposed method obtains the best values for the naturalness index, meaning that the produced recolored images maintain high quality in terms of the natural appearance when they are seen by a normal color vision viewer. However, there are some results (i.e. painting 2 in the protanopia experiment, painting 6 in the deuteranopia experiment, and painting 6 in the tritanopia experiment) where the proposed framework was outperformed by the method of Wong and Bishop [13]. Remarkably, even in these experimental simulations, it exhibited a behavior that is close enough to the respective behavior of the method in [13]. As far as the method of Huang et al [9] is concerned, its behavior is inferior in all experiments.

To continue the experimental evaluation of the algorithm, the feature similarity index (FSIMc) developed in [24] is studied. As the value of the index FSIMc increases the chrominance information of the recolored image is closer to the chrominance information of the original image.

Table 4: FSIMc index for the case of protanopia

Painting	Huang et al [9]	Wong and Bishop [13]	Proposed
Painting 1	0.9873	0.9439	**0.9911**
Painting 2	**0.9918**	0.9830	0.9876
Painting 3	0.9670	0.9422	**0.9891**
Painting 4	0.9816	0.9653	**0.9903**
Painting 5	0.9779	0.9700	**0.9915**
Painting 6	0.9644	0.9347	**0.9883**

Tables 4-6 illustrate the FSIMc values obtained by the three methods for all dichromacy cases and all paintings. As indicated by the above tables, apart from some experimental cases (i.e. painting 2 in the protanopia experiment, paintings 2 and 6 in the deuteranopia experiment, and paintings 3 and 6 in the tritanopia experiment), the proposed algorithm achieves the best results in most of the simulations, which directly implies that the recolored paintings look similar to the original ones.

Table 5: FSIMc index for the case of deuteranopia

Painting	Huang et al [9]	Wong and Bishop [13]	Proposed
Painting 1	0.9927	0.9439	**0.9935**
Painting 2	0.9830	**0.9976**	0.9926
Painting 3	0.9466	0.9422	**0.9926**
Painting 4	0.9916	0.9653	**0.9954**
Painting 5	0.9880	0.9700	**0.9920**
Painting 6	**0.9722**	0.9347	0.9589

Table 6: FSIMc index for the case of tritanopia

Painting	Huang et al [9]	Wong and Bishop [13]	Proposed
Painting 1	0.9328	0.9461	**0.9500**
Painting 2	0.9313	0.9386	**0.9731**
Painting 3	**0.9803**	0.9535	0.9144
Painting 4	0.9743	0.8895	**0.9838**
Painting 5	0.9652	0.9228	**0.9747**
Painting 6	0.9690	**0.9953**	0.9300

The next experiment concerns the visual comparison of the three algorithms. Figures 7-10 report some of the results.

Figure 7: Results on Painting 5 for the case of Protanopia: (a) recolored (method of Wong et al [13]), (b) recolored as seen by a protanope (method of Wong et al [13]), (c) recolored (proposed method), (d) recolored as seen by a protanope (proposed method); Results on Painting 6 for the case of Protanopia: (e) recolored (method of Huang et al [9]), (f) recolored as seen by a protanope (method of Huang et al [9]), (g) recolored (proposed method), (h) recolored as seen by a protanope (proposed method).

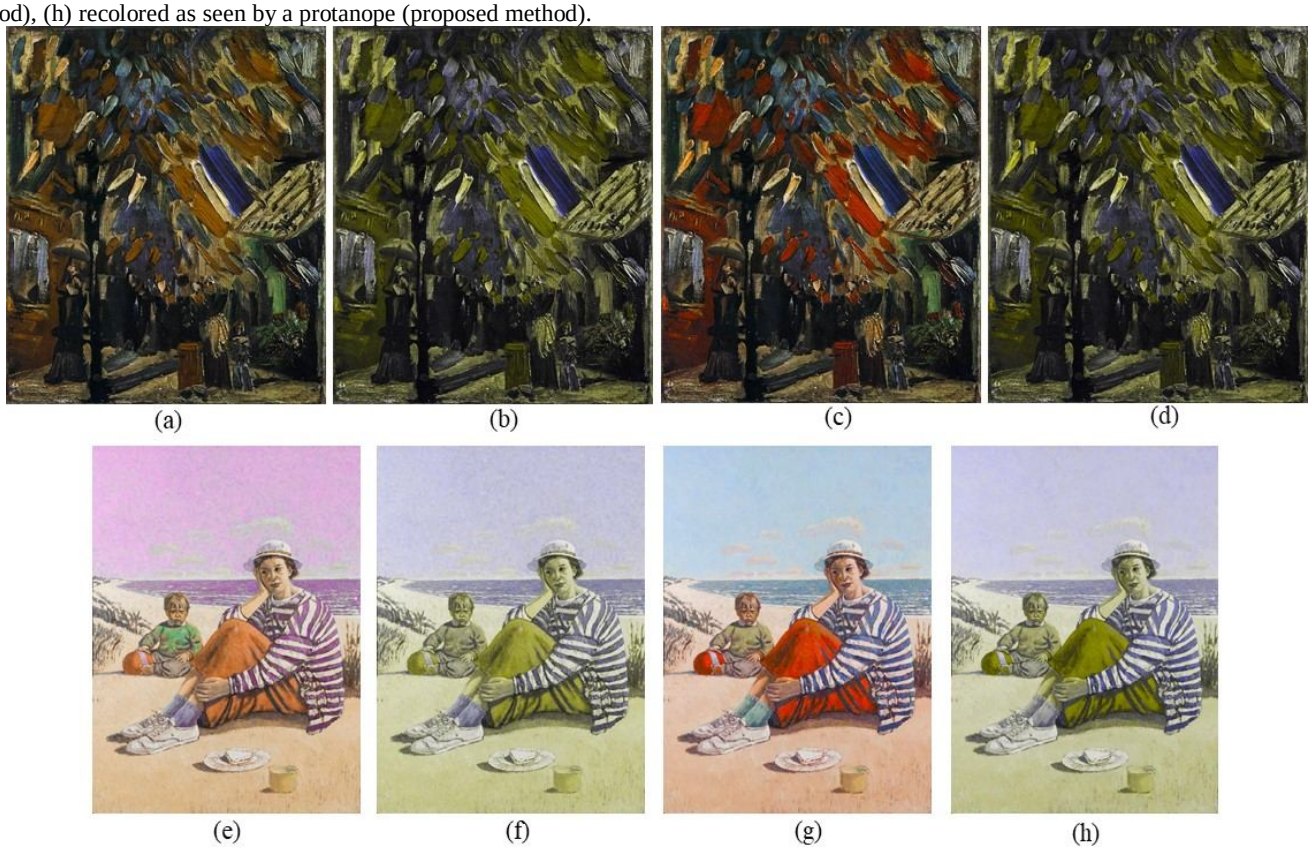

Figure 8: Results on Painting 2 for the case of Deuteranopia: (a) recolored (method of Huang et al [9]), (b) recolored as seen by a deuteranope (method of Huang et al [9]), (c) recolored (proposed method), (d) recolored as seen by a deuteranope (proposed method); Results on Painting 4 for the case of Deuteranopia: (e) recolored (method of Wong et al [13]), (f) recolored as seen by a deuteranope (method of Wong et al [13]), (g) recolored (proposed method), (h) recolored as seen by a deuteranope (proposed method).

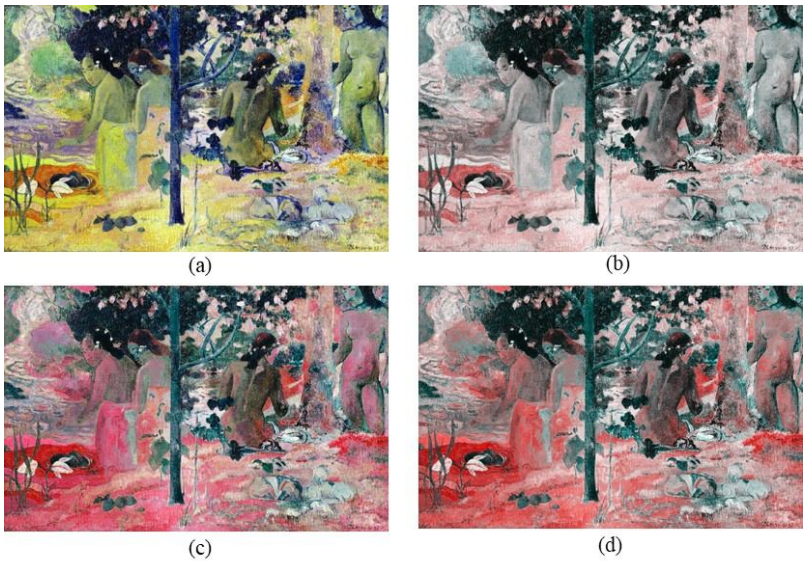

Figure 9: Results on Painting 1 for the case of Tritanopia: (a) recolored (method of Wong et al [13]), (b) recolored as seen by a tritanope (method of Wong et al [13]), (c) recolored (proposed method), (d) recolored as seen by a tritanope (proposed method).

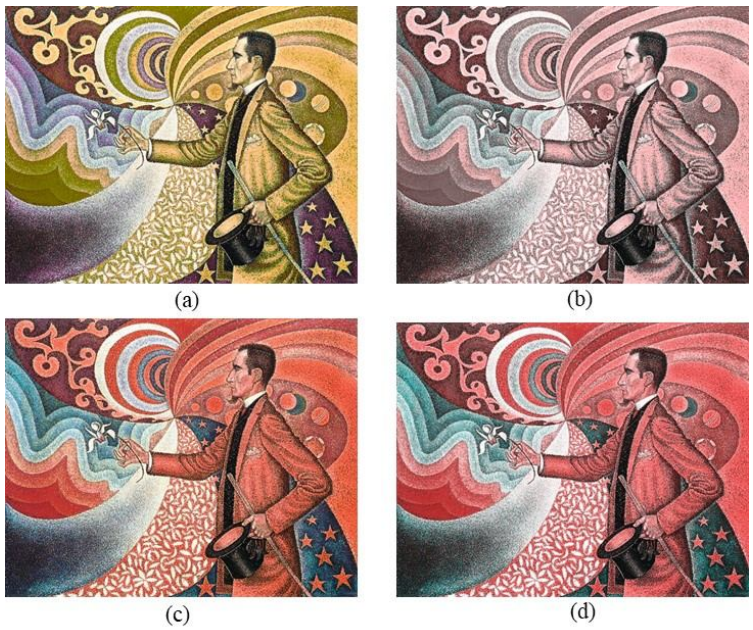

Figure 10: Results on Painting 3 for the case of Tritanopia: (a) recolored (method of Huang et al [9]), (b) recolored as seen by a tritanope (method of Huang et al [9]), (c) recolored (proposed method), (d) recolored as seen by a tritanope (proposed method).

Specifically, Figure 7 depicts some results for protanopia, where the proposed method is compared to the method developed in [13] for the painting 5, and the method in [9] for the painting 6. Figure 8 illustrates some results obtained for deuteranopia, where our algorithm is compared to the method in [9] for the painting 2, and the method in [13] for the painting 4. Figure 9 presents the results for painting 1, where the proposed methodology is compared to the method of Wong et al [13] considering the tritanopia deficiency. Finally, Figure 10 reports the respective results for the painting 3 considering the case of tritanopia, where the proposed method is compared to the method of Huang et al [9].

In view of the respective images in Figures 2 and 3, it can be easily seen that the recolored images, obtained by the proposed method in Figures 7-10, look more similar to the original images than the recolored images from the other two recoloring methods. These results are quite convincing and are supported by the numerical results reported in Tables (1)-(6).

The main outcomes of the above experiments indicate that the naturalness index and the FSIMc index are effectively optimized by the proposed approach. In addition, the contrast of the original image is sufficiently retained by the recolored image, while the method can naturally modify the original colors enhancing the perception of color-blind viewers.

4. CONCLUSIONS

In this paper an effective algorithmic framework was proposed to perform recoloring of art paintings. The goal was to enhance the color perception of people suffering from dichromacy. All cases of dichromacy, i.e. protanopia, deuteranopia, and tritanopia, were studied. The methodology involved three standard color spaces namely, the RGB, the CIELab, and the LMS space. To reduce the computational time, the colors of the original image were clustered. The resulting cluster centers (which are colors) were simulated by a standard model to approximate the dichromacy color vision deficiency. Then, colors that are confused by the color-blind were embedded in an objective function, the minimization of which estimated the parameters that decide the recoloring strategy.

The method was tested in several experimental cases. The main findings of the experiments can be enumerated as follows: (a) the naturalness of the recolored image is preserved when it is compared to the original image, indicating that the recolored image is naturally perceived by a normal color vision viewer; (b) the contrast is sufficiently retained by the recolored image; (c) the colors in the recolored image can easily be distinguished by the color-blind.

Future efforts could extend the present algorithm by developing more sophisticated learning approaches and effective color transformations to improve the color perception by viewers that suffer from dichromacy and anomalous trichromacy.

ACKNOWLEDGEMENT

This research is co-financed by Greece and the European Union (European Social Fund-ESF) through the Operational Programme "Human Resources Development, Education and Lifelong Learning 2014-2020" in the context of the project "Color perception enhancement in digitized art paintings for people with Color Vision Deficiency" (MIS 5047115).

REFERENCES

1. Stockman, L. T. Sharpe, "**The spectral sensitivities of the middle- and long-wavelength-sensitive cones derived from measurements in observers of known genotype**" *Vision Research*, Vol. 40, pp. 1711–1737, 2000. https://doi.org/10.1016/S0042-6989(00)00021-3
2. H. Brettel, F. Vienot, J. D. Mollon, "**Computerized simulation of color appearance for dichromats**", *Journal of the Optical Society of America A*, Vol. 14(10), pp. 2647-2655, 1997.
3. M. Ribeiro, A. J. Gomes, "**Recoloring algorithms for colorblind people: A survey**", *ACM Computing Surveys*, Vol. 52(4), pp. 72:1-72:37, 2019. https://doi.org/10.1145/3329118
4. J.-B. Huang, Y.-C. Tseng, S.-I. Wu, S.-J. Wang, "**Information preserving color transformation for protanopia and deuteranopia**", *IEEE Signal Processing Letters*, Vol. 14 (10), pp. 711-714, 2007.
5. J.-Y. Jeong, H.-J. Kim, T.-S. Wang, Y.-J. Yoon, S.-J. Ko, "**An efficient re-coloring method with information preserving for the color-blind**", *IEEE Transactions on Consumer Electronics*, Vol. 57 (4), pp. 1953-1960, 2011.
6. R. Sayal, C. Subbalakhmi, H. S. Saini, "**Mobile App accessibility for visually impaired**", *International Journal of Advanced Trends in Computer Science and Engineering*, Vol. 9(1), pp. 182-185, 2020. https://doi.org/10.30534/ijatcse/2020/27912020
7. M. F. Hassan, R. Paramesran, "**Naturalness preserving image recoloring method for people with red–green deficiency**", *Signal Processing: Image Communication* Vol. 57, pp. 126–133, 2017.
8. L. Jefferson, R. Harvey, "**Accommodating color blind computer users**", *In the Proceedings of the 8th international ACM SIGACCESS conference on Computers and accessibility* (Assets '06), pp. 40-47, 2006.
9. J.-B. Huang, C.-S. Chen, T.-S. Jen, S.-J. Wang, "**Image recolorization for the color blind**", *In the Proceedings of the 2009 IEEE International Conference on Acoustics, Speech and Signal Processing* (ICASSP 2009), pp. 1161-1164, 2009.
10. G. E. Tsekouras, S. Chatzistamatis, C. N. Anagnostopoulos, D. Makris, "**Color adaptation for protanopia using differential evolution-based fuzzy clustering: A case study in digitized paintings**", *In the Poceedings of the 2018 IEEE Conference on Evolving and Adaptive Intelligent Systems* (EAIS 2018), 2018.
11. S. Chatzistamatis, A. Rigos, G. E. Tsekouras, "**Image Recoloring of Art Paintings for the Color Blind Guided by Semantic Segmentation**", *In the Proceedings of the 21st International Conference on Engineering Applications of Neural Networks* (EANN 2020), pp. 261-273, 2020. https://doi.org/10.1007/978-3-030-48791-1_20
12. H.-Y. Lin, L.-Q. Chen, M.-L. Wang, "**Improving discrimination in color vision deficiency by image re-coloring**" *Sensors*, 19, 2250, 2019; doi:10.3390/s19102250.
13. A. Wong, W. Bishop, "**Perceptually-adaptive color enhancement of still images for individuals with dichromacy**", *In the Proceedings of the 21st Canadian Conference on Electrical and Computer Engineering*, 2008.
14. R. Johnston-Feller, "**Color science in the examination museum objects**", Getty Conservation Institute, Los Angeles, 2001.
15. G. W. Ho, "**Color, vision, and art: teaching, learning, and making art with color blind awareness**", MsC Thesis, University of Florida, 2014.

16. M. F. Marmor, P. Lanthony, "**The dilemma of color deficiency and art**", *Survey of Ophthalmology*, Vol. 45 (5), pp. 407-414, 2001.
17. M. D. Fairchild, "**Color appearance models**", Wiley, U.K., 2005.
18. R.W.G. Hunt, M.R. Pointer, "**Measuring Colour**", 4th Edition, Wiley, U. K., 2011.
19. C. Poynton, "**Digital Video and HDTV Algorithms and Interfaces**", Morgan Kaufmann Publishers, San Francisco, 2003.
20. M. Anwar, F. Mustapha, N. Ibrahim, M. T. H. Sutan, I. A. Halin, F. Bobby, S. Nazrin W. AbduRahman, M. I. Hassim, "**Comparative study of composite defect and segmentation in RGB and Lab colour space**", *International Journal of Advanced Trends in Computer Science and Engineering*, Vol. 8(1), pp. 455-459, 2019. https://doi.org/10.30534/ijatcse/2019/6681.62019
21. M. Karthikeyan, A. Arivarasan, D. Kumaresan, "**Performance assessment of various text document features through k-means document clustering approach**", *International Journal of Advanced Trends in Computer Science and Engineering*, Vol. 8(85), pp. 1969-1977, 2019.
22. M. Shenify, "**Understanding user's behavior by social media data clustering**", *International Journal of Advanced Trends in Computer Science and Engineering*, Vol. 9(1), pp. 167-170, 2020. https://doi.org/10.30534/ijatcse/2019/21852019
23. K. V. Price, R. M. Storn, J. A. Lampinen, "**Differential evolution: a practical approach to global optimization**" Springer-Verlag, 2005.
24. L. Zhang, L. Zhang, X. Mou, D. Zhang, "**FSIM: A feature similarity index for image quality assessment**", *IEEE Transactions on Image Processing*, Vol. 20 (8), pp. 2378-2386, 2011. https://doi.org/10.1109/TIP.2011.2109730